TECHNICAL NOTES

NATIONAL ADVISORY COMMITTEE FOR AERONAUTICS

No. 697

THE FREQUENCY OF TORSIONAL VIBRATION OF A TAPERED BEAM

By Robert P. Coleman
Langley Memorial Aeronautical Laboratory

Washington
March 1939

NATIONAL ADVISORY COMMITTEE FOR AERONAUTICS

TECHNICAL NOTE NO. 697

THE FREQUENCY OF TORSIONAL VIBRATION OF A TAPERED BEAM

By Robert P. Coleman

SUMMARY

A solution for the equation of torsional vibration of tapered beams has been found in terms of Bessel functions for beams satisfying the following conditions: (a) The cross sections along the span are similar in shape; and (b) the torsional stiffness of a section can be expressed as a power of a linear function of distance along the span. The method of applying the analysis to actual cases has been described. Charts are given from which numerical values can be immediately obtained for most cases of practical importance. The theoretical values of the frequency ratio have been experimentally checked on five beams having different amounts of taper.

INTRODUCTION

The frequency of torsional vibration of a uniform beam can be calculated for a number of shapes of cross section. (See references 1 and 2.) The corresponding cases of tapered beams either have not been solved or are not readily available. A special case of longitudinal vibration of tapered beams treated by Nabl (reference 3) is applicable also to torsion for a special case ($n = 2$). In the present paper, the analysis has been extended to the case of tapered beams subject to rather broad conditions, and a closed solution of the differential equation of motion has been obtained in terms of Bessel functions. The result is expressed in such a form that the effect of taper is given independently of the effect of cross section. Hence, except for certain limitations imposed on the solution of the differential equation, the frequency of a tapered beam can be calculated if the solution for the corresponding uniform beam is known.

SYMBOLS

θ, angular displacement from equilibrium.

x, y, z, rectangular coordinates in beam.

I_p, polar moment of inertia of section.

J, torsion modulus of section.

G, shear modulus of material.

l, length of beam.

t, time.

ρ, density of material.

ω, angular frequency ($\omega = 2\pi f$, where f is in cycles per second).

ω_1, angular frequency of a uniform beam, $\frac{\pi}{2l}\sqrt{\frac{GJ}{\rho I_p}}$

φ, torsion function.

A, B, C_1, C_2, constants.

n, exponent in expression for variation of torsion modulus along span ($n = 2\lambda + 1$).

$\lambda = (n - 1)/2$.

c, semichord.

$\eta = \left(\frac{c}{c_o}\right)^{4/n}$

$\xi = \frac{z}{l}$

$\zeta_o = \frac{l\omega}{(1 - \eta_t)}\sqrt{\frac{I_p\rho}{JG}} = \frac{1}{1 - \eta_t}\frac{\omega}{\omega_1}\frac{\pi}{2}$

ζ_r, roots of equation (7).

$\zeta = \eta \zeta_o$

$\beta = \sqrt{\frac{I_p \rho}{JG}}$

m, number of mode.

$J_\lambda(\zeta), Y_\lambda(\zeta)$, Bessel functions of first and second kind, respectively.

Subscripts:

o, at root.

t, at tip.

ANALYSIS

The differential equation for the motion of a section of a beam in torsional vibration (reference 1) is

$$\rho I_p \frac{\partial^2 \theta}{\partial t^2} = \frac{\partial}{\partial z}\left[GJ(z) \frac{\partial \theta}{\partial z}\right] \tag{1}$$

where GJ is the torsional rigidity of the section. For harmonic vibrations it is known that

$$\frac{\partial^2 \theta}{\partial t^2} = - \omega^2 \theta$$

Then

$$\frac{d}{dz}\left[GJ(z) \frac{d\theta}{dz}\right] + \rho \omega^2 I_p \theta = 0$$

or

$$\frac{d^2\theta}{dz^2} + \frac{1}{J}\frac{dJ}{dz}\frac{d\theta}{dz} + \frac{I_p \rho \omega^2 \theta}{JG} = 0 \tag{2}$$

The functions I_p and J (reference 4) for a prismatic beam may be expressed in the form

$$I_p = \iint (x^2 + y^2)\, dx\, dy$$

$$J = \iint \left(x^2 + y^2 + x\frac{\partial \varphi}{\partial y} - y\frac{\partial \varphi}{\partial x}\right) dx\, dy$$

where φ, the torsion function, depends upon the cross section. This function is known for a number of shapes of cross section. A few examples from references 5 and 6 are given:

(a) Circle of radius r:

$$\varphi = 0, \quad J = I_p = (\pi r^2)\frac{r^2}{2}$$

(b) Ellipse with semiaxes a and b:

$$\varphi = -\frac{a^2 - b^2}{a^2 + b^2} xy, \quad J = (\pi ab)\frac{a^2 b^2}{a^2 + b^2}$$

(c) Rectangle with sides 2a and 2b:

$$\varphi = -xy + 4b^2 \left(\frac{2}{\pi}\right)^3 \sum_{n=0}^{\infty} \frac{(-)^n \sinh \frac{(2n+1)\pi x}{2b}}{(2n+1)^3 \cosh \frac{(2n+1)\pi a}{2b}} \sin \frac{(2n+1)\pi y}{2b}$$

$$J = \frac{16}{3} k\, ab^3$$

where k has the values given by the following table.

a/b	1.00	1.50	1.75	2.00	2.50	3.00	4	6	8	10	∞
k	.424	.589	.642	.688	.748	.790	.844	.896	.922	.940	1

The torsion modulus, J, of a section of a tapered beam is very nearly the same as that of a prismatic beam having the same section. A comparison of the angular deflections produced by a static torque in a conical shaft as calculated by the exact theory (reference 7) and by in-

tegrating the torsion modulus for a cylindrical shaft shows a discrepancy of the order of $1/6 \tan^2 \alpha$, where α is the half angle of the cone. For a cone with $\tan \alpha = 0.10$, the discrepancy is only 0.17 percent. In the following analysis, this distinction in the torsion modulus has been ignored.

The boundary conditions to be applied to the solution of equation (2) will depend upon the method of support of the beam. For the case of most interest in this paper, a beam built in at $z = 0$ and free at $z = l$, the boundary conditions are:

$$\text{at} \quad z = 0, \quad \theta = 0$$

$$\text{at} \quad z = l, \quad \frac{\partial \theta}{\partial z} = 0$$

A solution of equation (2) has been found for the case of tapered beams satisfying the following conditions:

(a) All cross sections along the span are similar in shape.

(b) The torsion modulus J can be expressed as a power of a linear function of position along the span. Then, from condition (a), the ratio I_p/J is a constant along the span and is equal to its value at the root section, I_{p_o}/J_o. From condition (b),

$$J = J_o(1 - Bz)^n = J_o \eta^n$$

The torsion modulus is proportional to the fourth power of the linear dimensions. Hence, in terms of the semichord,

$$\eta^n = \frac{J}{J_o} = \left(\frac{c}{c_o}\right)^4$$

$$\eta = \left(\frac{c}{c_o}\right)^{4/n}$$

At the tip,

$$\eta_t = \left(\frac{c_t}{c_o}\right)^{4/n} \tag{3}$$

It may be noted that

$$B = \frac{1 - \eta_t}{l}$$

Figure 1 shows a number of typical plan forms corresponding to different values of n. The upper half of this figure can also be considered as a plot of semichord against η for different values of n. In this case η increases from right to left. The following properties of these curves are noted:

$$\text{at} \quad \eta = 1, \quad \frac{d\, c/c_o}{d\, \eta} = \frac{n}{4}$$

$$\text{at} \quad \eta = 0, \quad \frac{d\, c/c_o}{d\, \eta} = 0 \quad \text{when} \quad n > 4$$

$$= \infty \quad \text{when} \quad n < 4$$

In terms of ξ and β, equation (2) can be written

$$\frac{d^2\theta}{d\xi^2} + \frac{1}{J}\frac{dJ}{d\xi}\frac{d\theta}{d\xi} + \omega^2 \beta^2 l^2 \theta = 0$$

For the case of a uniform beam $(dJ/d\xi = 0)$, equation (2) has the well-known solution

$$\theta = C_1 \sin \beta \omega l \xi + C_2 \cos \beta \omega l \xi$$

The frequency equation for a cantilever beam is

$$\cos \beta \omega l = 0$$

$$\beta \omega l = (2m - 1)\frac{\pi}{2}$$

where $m = 1, 2, 3, \ldots$

The lowest frequency is

$$\omega_1 = \frac{\pi}{2\beta l}$$

Equation (2) can then be written

$$\frac{d^2\theta}{d\xi^2} + \frac{1}{J}\frac{dJ}{d\xi}\frac{d\theta}{d\xi} + \left(\frac{\omega}{\omega_1}\frac{\pi}{2}\right)^2 \theta = 0 \qquad (4)$$

Now

$$\eta = 1 - B\,l\,\xi$$

$$B = \frac{1 - \eta}{l\,\xi} = \frac{1 - \eta_t}{l}$$

$$\xi = \frac{1 - \eta}{1 - \eta_t}$$

$$\frac{d}{d\xi} = \frac{d}{d\eta}\frac{d\eta}{d\xi} = -\left(1 - \eta_t\right)\frac{d}{d\eta}$$

After equation (4) has been expressed in terms of η, it becomes

$$\left(1 - \eta_t\right)^2 \frac{d^2\theta}{d\eta^2} + \left(1 - \eta_t\right)^2 \frac{n}{\eta}\frac{d\theta}{d\eta} + \left(\frac{\omega\,\pi}{\omega_1\,2}\right)^2 \theta = 0$$

Put

$$\frac{\eta}{1 - \eta_t}\frac{\omega\,\pi}{\omega_1\,2} = \zeta = \eta\,\zeta_o$$

Then

$$\frac{d^2\theta}{d\zeta^2} + \frac{n}{\zeta}\frac{d\theta}{d\zeta} + \theta = 0 \qquad (5)$$

SOLUTION OF DIFFERENTIAL EQUATION

A solution of equation (5) has been found in terms of Bessel functions. Put

$$\theta = \frac{1}{\zeta^\lambda} J_\lambda(\zeta)$$

Then equation (5) becomes

$$\frac{1}{\zeta^\lambda}\left[\frac{d^2J(\zeta)}{d\zeta^2} + \frac{n - 2\lambda}{\zeta}\frac{dJ(\zeta)}{d\zeta} + \left(1 - \frac{\lambda n - \lambda(\lambda+1)}{\zeta^2}\right) J(\zeta)\right] = 0$$

If $\lambda = (n - 1)/2$, this equation reduces to Bessel's equation:

$$\frac{d^2J(\zeta)}{d\zeta^2} + \frac{1}{\zeta}\frac{dJ(\zeta)}{d\zeta} + \left(1 - \frac{\lambda^2}{\zeta^2}\right) J(\zeta) = 0$$

Therefore $J_\lambda(\zeta)$ is a Bessel function of order λ.

The complete solution containing two arbitrary constants to be determined by the boundary conditions is

$$\left.\begin{aligned} \theta &= \frac{1}{\zeta^\lambda}\left[AJ_\lambda(\zeta) + BJ_{-\lambda}(\zeta)\right]; \quad \lambda, \text{ nonintegral} \\ \theta &= \frac{1}{\zeta^\lambda}\left[AJ_\lambda(\zeta) + BY_\lambda(\zeta)\right]; \quad \lambda, \text{ integral} \end{aligned}\right\} \quad (6)$$

The function $Y_\lambda(\zeta)$ is a Bessel function of the second kind.

The boundary conditions in terms of ζ are:

at $z = 0$, $\zeta = \zeta_o$, $\theta = 0$

at $z = l$, $\eta = \eta_t$, $\zeta = \eta_t \zeta_o$, $\frac{d\theta}{d\zeta} = 0$

After these conditions have been applied, the resulting equations can be simplified by means of the relations for Bessel functions:

$$\frac{d}{dx}\left[x^{-n} J_n(x)\right] = -x^{-n} J_{n+1}(x)$$

$$\frac{d}{dx}\left[x^n J_n(x)\right] = x^n J_{n-1}(x)$$

The condition that the two equations for A and B have solutions other than $A = 0$, $B = 0$, is that the determinant of the coefficients of A and B vanish:

$$\left.\begin{aligned} &\begin{vmatrix} J_\lambda(\zeta_o) & J_{-\lambda}(\zeta_o) \\ J_{\lambda+1}(\eta_t\zeta_o) & -J_{-\lambda-1}(\eta_t\zeta_o) \end{vmatrix} = 0; \quad \lambda, \text{ nonintegral} \\ &\begin{vmatrix} J_\lambda(\zeta_o) & Y_\lambda(\zeta_o) \\ J_{\lambda+1}(\eta_t\zeta_o) & Y_{\lambda+1}(\eta_t\zeta_o) \end{vmatrix} = 0; \quad \lambda, \text{ integral} \end{aligned}\right\} \quad (7)$$

This condition determines an admissible set of values of ζ_o, the roots of equation (7). These roots will be called ζ_r.

After the value or values of ζ_o that satisfy the determinantal equation have been found, the shapes of the deflection curves for the various modes can be directly obtained from equation (6). At the root section, $\zeta = \zeta_o = \zeta_r$, $\theta = 0$,

$$0 = AJ_\lambda(\zeta_r) + BJ_{-\lambda}(\zeta_r); \quad \lambda, \text{ nonintegral}$$

$$0 = AJ_\lambda(\zeta_r) + BY_\lambda(\zeta_r); \quad \lambda, \text{ integral}$$

Hence

$$\left.\begin{aligned} \theta &= \frac{A}{\zeta^\lambda}\left[J_\lambda(\zeta) - \frac{J_\lambda(\zeta_r)}{J_{-\lambda}(\zeta_r)} J_{-\lambda}(\zeta)\right]; \quad \lambda, \text{ nonintegral} \\ \theta &= \frac{A}{\zeta^\lambda}\left[J_\lambda(\zeta) - \frac{J_\lambda(\zeta_r)}{Y_\lambda(\zeta_r)} Y_\lambda(\zeta)\right]; \quad \lambda, \text{ integral} \end{aligned}\right\} \quad (8)$$

where ζ determines position along the span.

Equation (7) is a transcendental equation of which the roots, ζ_r, determine the frequencies of the various modes. The equation cannot be solved explicitly but may be solved indirectly. The roots may be obtained to any desired accuracy by use of tables or by the graphical procedure of plotting the value of the determinant against ζ_o. For each root there is a corresponding natural frequency of vibration given by

$$\omega = \zeta_r \left(1 - \eta_t\right) \frac{2}{\pi} \omega_1$$

For the case of a pointed beam, equations (7) can be expressed in a simpler form. From the series expansion for Bessel functions,

$$\lim_{\eta_t \longrightarrow o} \frac{J_{\lambda+1}(\eta_t \zeta_o)}{J_{-\lambda-1}(\eta_t \zeta_o)} = \lim_{\eta_t \longrightarrow o} \frac{(\eta_t \zeta_o)^{2(\lambda+1)}}{2^{2(\lambda+1)}} \frac{\Gamma(-\lambda)}{\Gamma(\lambda+2)} = 0$$

Hence, for pointed beams ($\eta_t = 0$), the first of equations

(7) becomes

$$J_\lambda(\zeta_o) = -\frac{J_{\lambda+1}(\eta_t\zeta_o)}{J_{-\lambda-1}(\eta_t\zeta_o)} J_{-\lambda}(\zeta_o) = 0$$

When λ is an integer, the same result is obtained:

$$J_\lambda(\zeta_o) = \lim_{\eta_t \longrightarrow o} -\frac{J_{\lambda+1}(\eta_t\zeta_o)}{Y_{\lambda+1}(\eta_t\zeta_o)} Y_\lambda(\zeta_o)$$

$$= \lim_{\eta_t \longrightarrow o} \frac{(\eta_t\zeta_o)^{\lambda+1}}{2^{\lambda+1}(\lambda+1)!} \frac{\pi(\eta_t\zeta_o)^{\lambda+1}}{\lambda!\ 2^{\lambda+1}} Y_\lambda(\zeta_o)$$

$$= 0$$

APPLICATION OF ANALYSIS

The preceding analysis can be immediately applied to beams the forms of which are mathematically specified by values of n and η_t. Most beams, however, will not exactly correspond to one of these cases; a method must therefore be found for determining the best values of n and η_t for the actual beam. An approximate method will be illustrated for a wing the shape of which is given by a drawing. Other methods, such as the method of least squares, are also available for determining these parameters. The thickness will be assumed to vary in the same way as the plan form.

A sketch of a typical wing, together with a table of dimensions, is given in figure 2. It is required to represent this shape by an equation of the form

$$c = c_o\eta^{n/4}$$

The parameter η varies linearly along the span from a value of η_t at the tip to 1 at the root. The procedure is to assume arbitrarily a value of η_t, then to make a logarithmic plot of chord or semichord against η. This process is repeated for different values of η_t until the

value of η_t giving the best straight line is determined. The slope of this line is the value of $n/4$. The third and fourth columns of the table in figure 2 give values of η for the assumed values for η_t of 0 and 0.1. Figure 3 is a logarithmic plot of chord against η. The points for $\eta_t = 0$ fall nearly on a straight line. The slope of this line is 0.37, which gives $n = 4 \times 0.37 = 1.48$. The values of c recalculated from the equation

$$c = 0.96\ \eta^{0.37}$$

are given in the last column of the table in figure 2.

The frequency ratio, ω/ω_1, determined from the roots of equation (7), is a function of only two variables, n and η_t. Figure 4 shows this ratio as a function of η_t for several values of n. The actual frequency is given by

$$\omega = \left(\frac{\omega}{\omega_1}\right) \frac{\pi}{2l} \sqrt{\frac{JG}{I_p \rho}}$$

The frequency ratio for pointed beams ($\eta_t = 0$) is given in figure 5 for several values of n and for several modes. For the wing previously described (fig. 2), the frequency ratio is 1.77. The shape of the deflection curve is shown in figure 6 for several typical values of n and η_t.

EXPERIMENTAL RESULTS

Five duralumin beams (fig. 7) were constructed and their frequencies were measured to check the theoretical values of the frequency ratio. The central cross section of each beam was a rectangle 6 inches wide and 1/4 inch thick. The beams were geometrically similar in cross section along the span and had straight taper, the corresponding values of η_t being 1.00, 0.75, 0.50, 0.25, 0.00. It is apparent from the boundary conditions that a freely suspended symmetrical beam vibrating in torsion with a node at the center will have the same frequencies as one built in at the center. The preceding analysis may therefore be applied to these beams.

The experimental values of the frequency ratio are

plotted together with the theoretical curve for $n = 4$ in figure 8. The greatest discrepancy between experiment and theory is 2 percent, which is considered to be within the limit of accuracy determined by the machining of the beams and the measurements of the frequency.

CONCLUSIONS

The results of the tests of five beams showed that the assumptions underlying the equation of torsional vibration of a tapered beam

$$\rho I_p \frac{\partial^2 \theta}{\partial t^2} = \frac{\partial}{\partial z}\left[GJ(z)\frac{\partial \theta}{\partial z}\right]$$

are justifiable for all practical purposes. The frequency ratio for even the most tapered case agreed with the theory to within the experimental error.

Langley Memorial Aeronautical Laboratory,
National Advisory Committee for Aeronautics,
Langley Field, Va., January 23, 1939.

REFERENCES

1. Pfeiffer, F.: Torsionsschwingungen. Bd. VI, Kap. 4, Ziff. 34 des Handbuch der Physik, H. Geiger und Karl Scheel, Herausg., Julius Springer (Berlin), 1928, S. 358.

2. Schulze, F. A.: Über drehende Schwingungen von dünnen Stäben mit rechteckigen Querschnitte und ihre Verwendung zur Messung der Elastizitatskonstanten. Ann. d. Phys. (4), Bd. 13, 1904, S. 583.

3. Nabl, Joseph: Über die Longitudinalschwingungen von Stäben mit veranderlichen Querschnitte. Wiener Berichte, Bd. 111, 1902, S. 846-854.

4. Southwell, R. V.: An Introduction to the Theory of Elasticity. Clarendon Press (Oxford), 1936, p. 323.

5. Love, A. E. H.: A Treatise on the Mathematical Theory of Elasticity. 3d ed., University Press (Cambridge), 1920, p. 322.

6. Timoshenko, S.: Strength of Materials. Part I, 3d ed., D. Van Nostrand Co., Inc., 1936, pp. 77 and 80.

7. Timoshenko, S.: Theory of Elasticity. McGraw-Hill Book Co., Inc., 1934, p. 276.

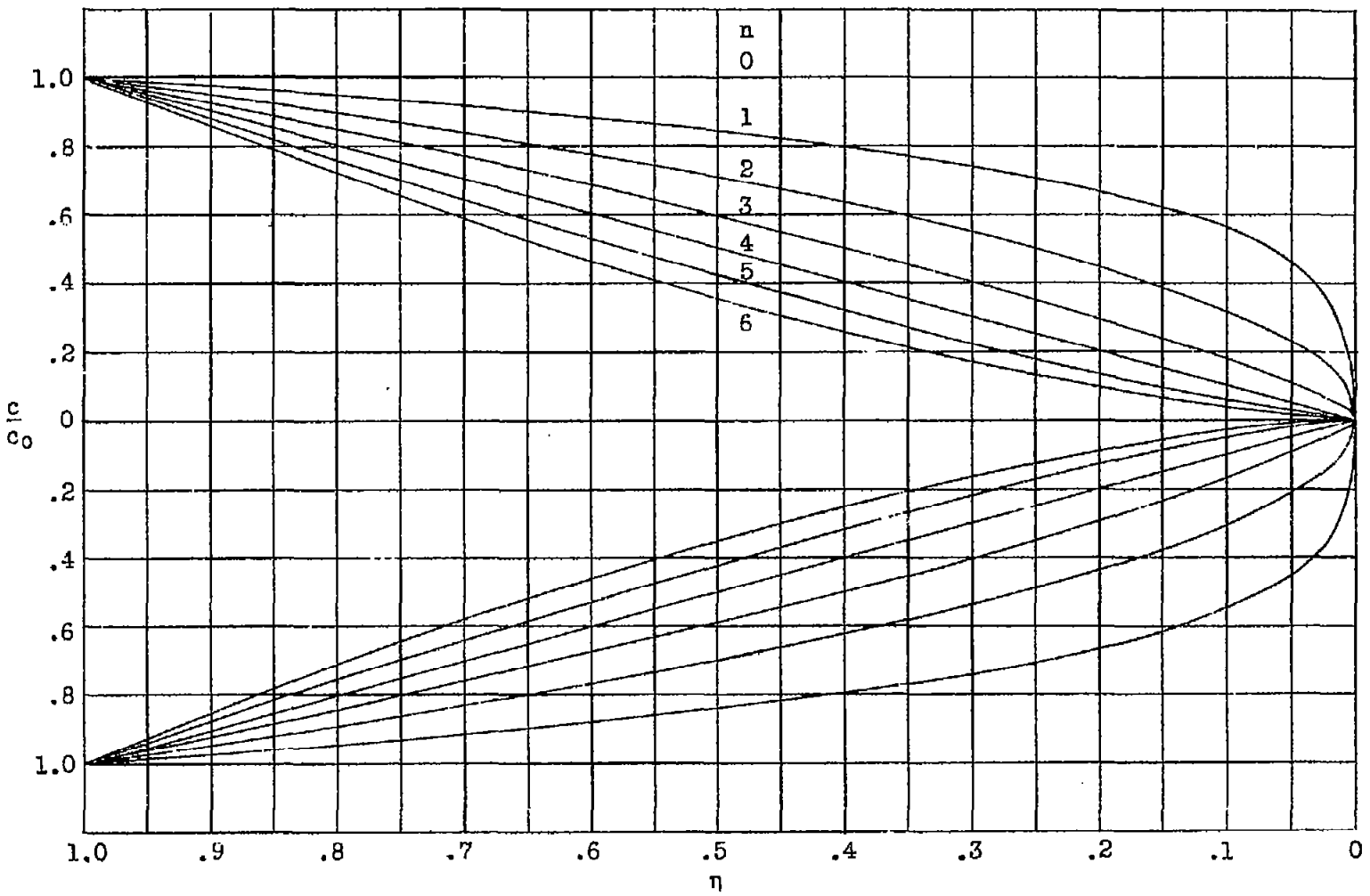

Figure 1.- Typical plan forms corresponding to different values of n.

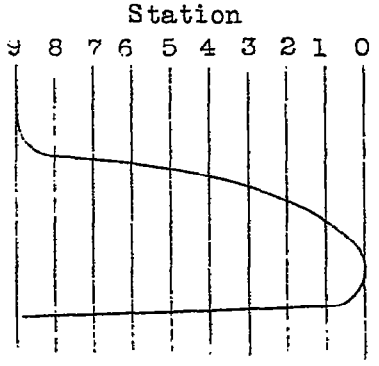

Station	Chord	η		$0.96\,\eta^{0.37}$
		$\eta_t = 0$	$\eta_t = 0,1$	
0	0.00	0.00	0.10	0.00
1	.46	.11	.20	.42
2	.57	.22	.30	.55
3	.65	.33	.40	.64
4	.72	.44	.50	.71
5	.77	.55	.60	.76
6	.80	.66	.70	.82
7	.82	.77	.80	.87
8	.85	.88	.90	.91
9	.98	.99	1.00	.96

Figure 2.- Plan of a typical wing.

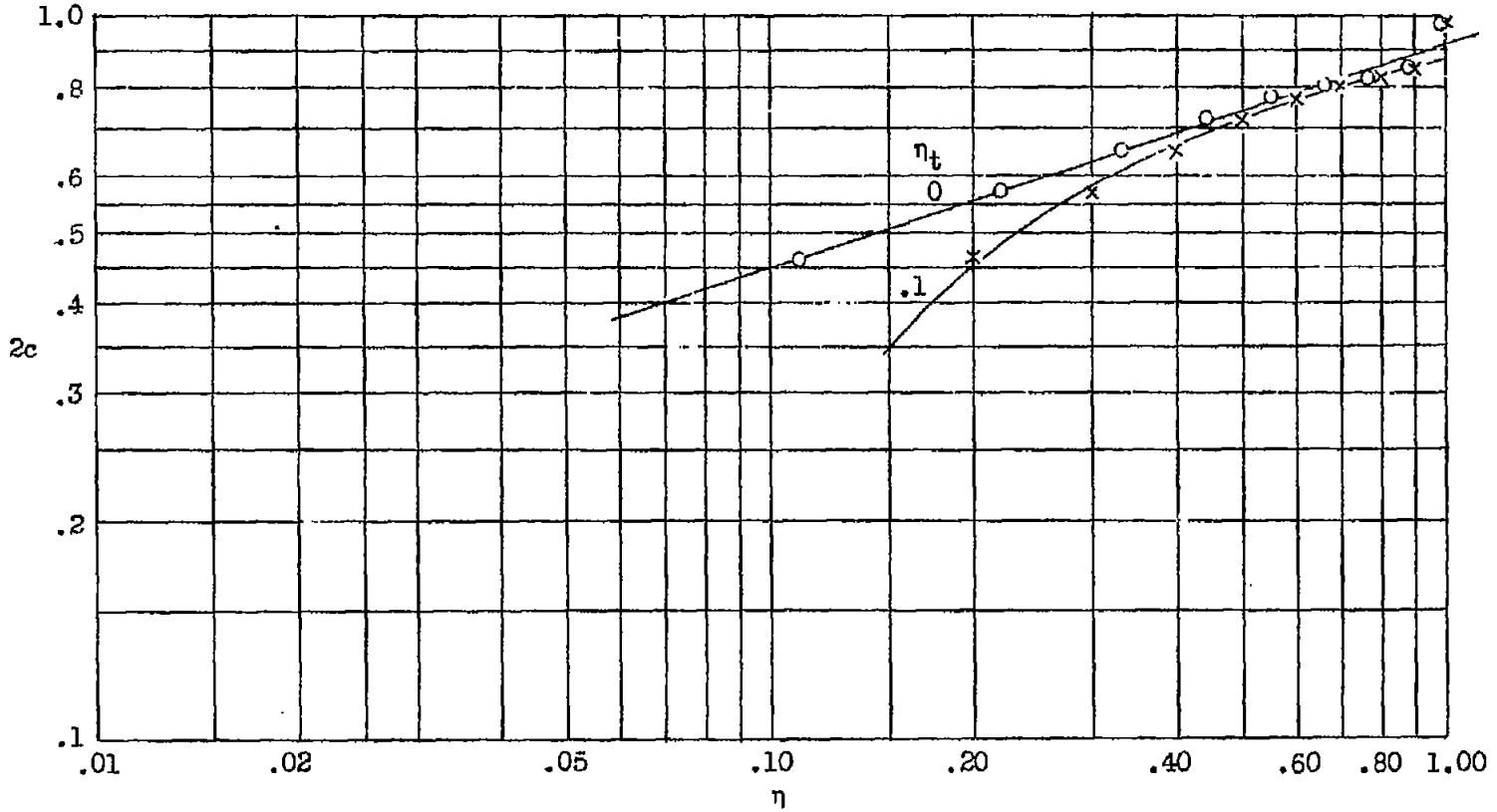

Figure 3.- Logarithmic plot of chord against η for a typical wing.

Fig. 4

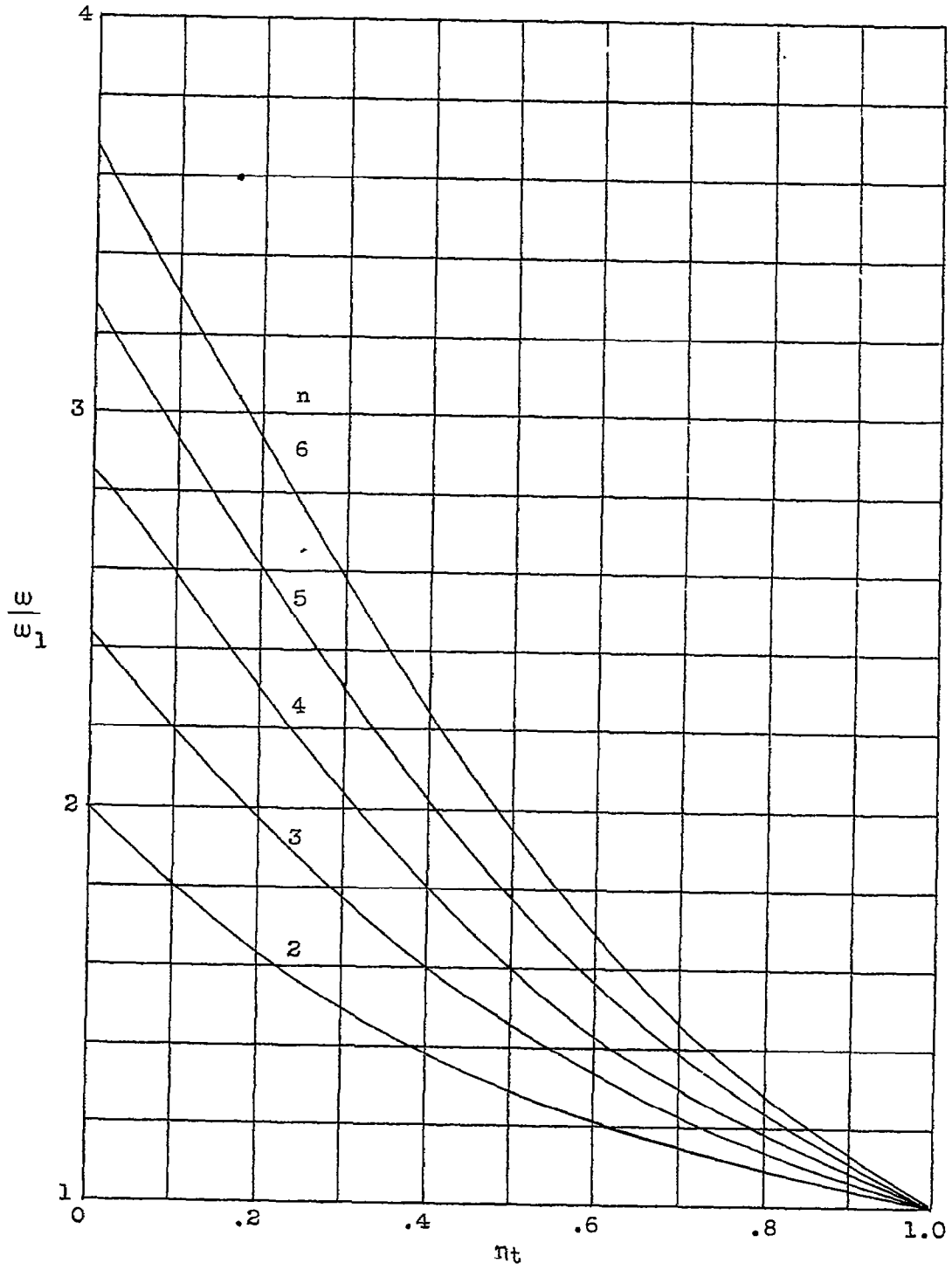

Figure 4.- The frequency ratio ω/ω_1, as a function of η_t

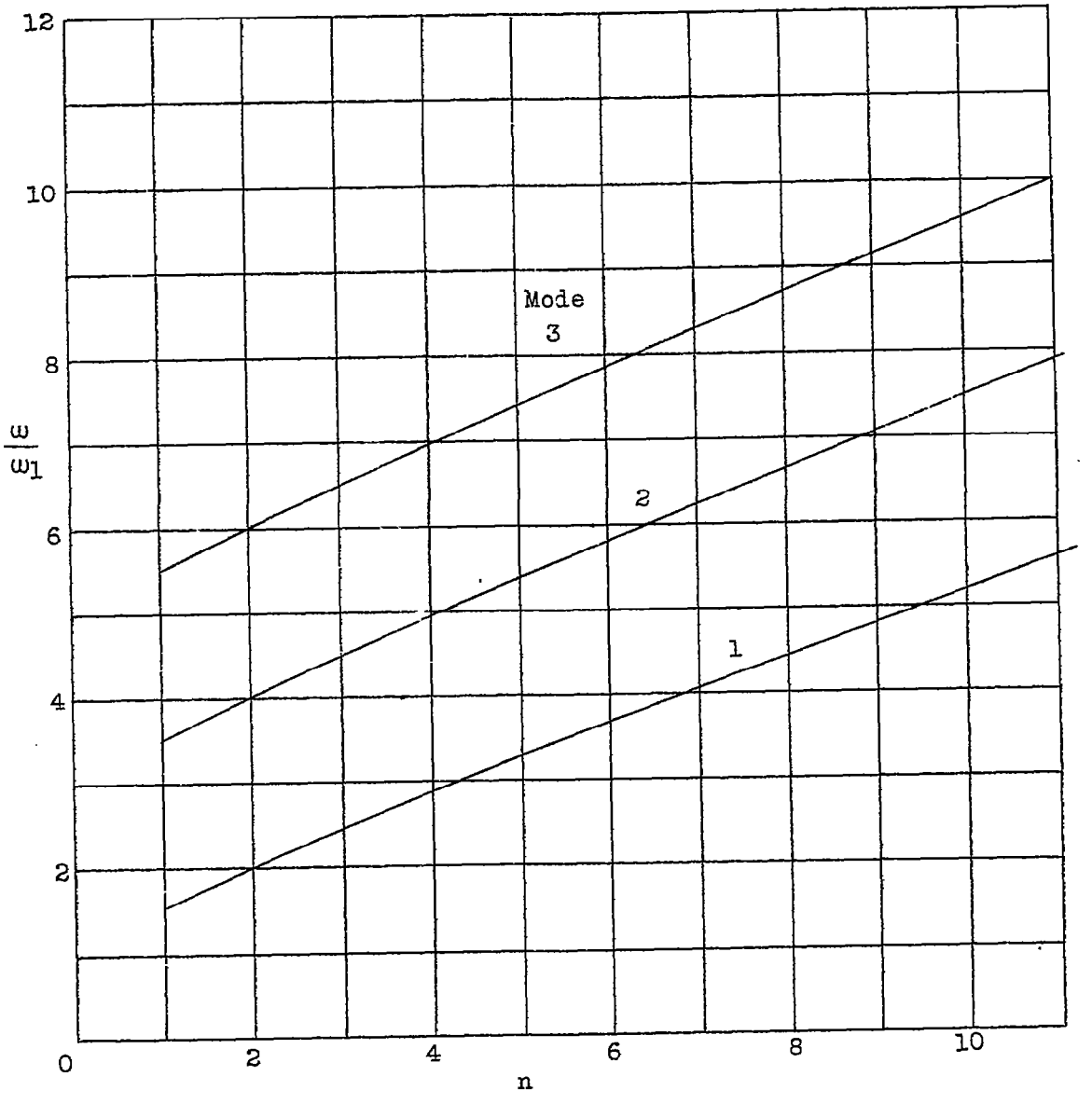

Figure 5.- The frequency ratio, ω/ω_1, for pointed beams ($\eta_t = 0$).

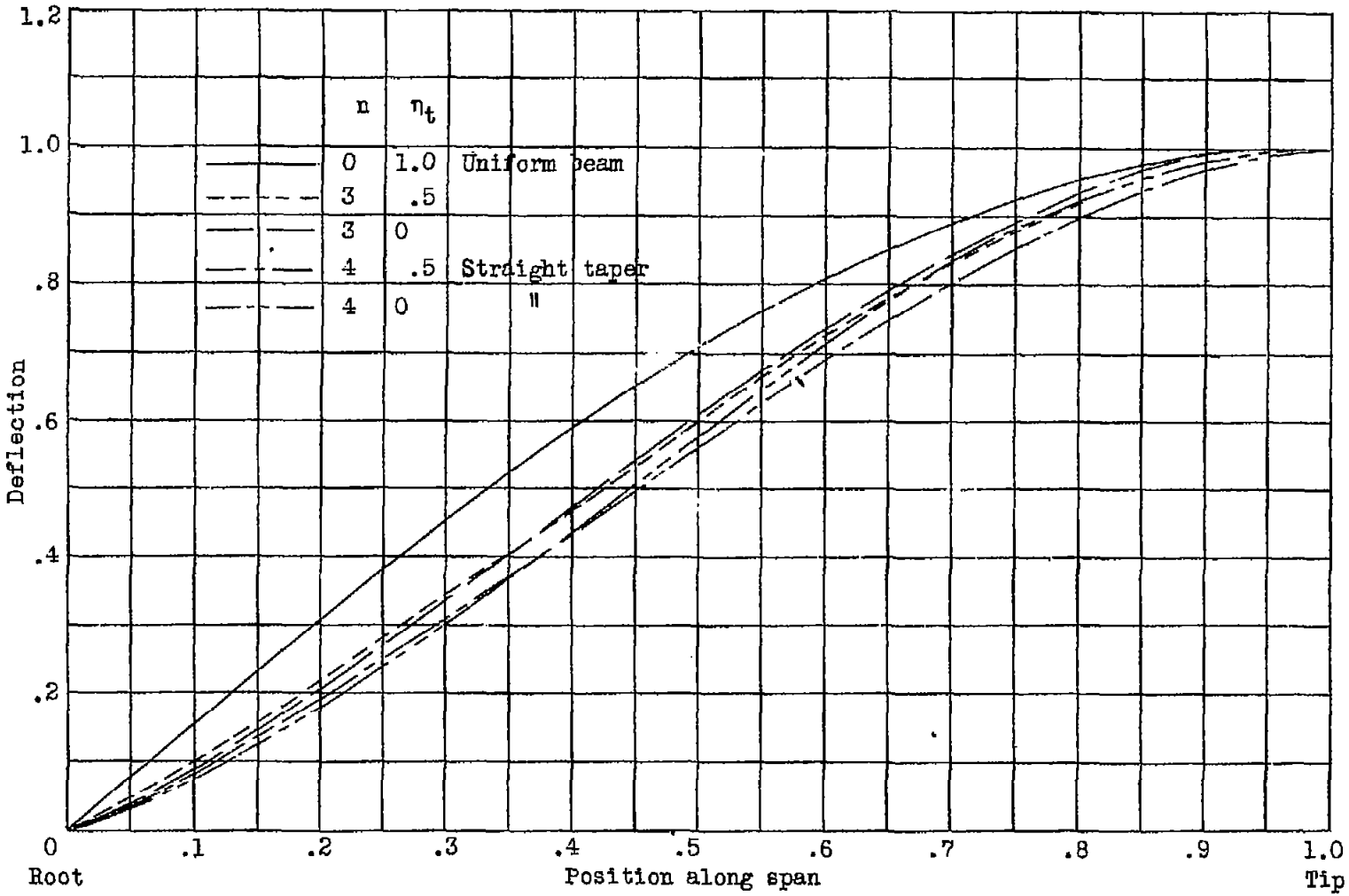

Figure 6.- The shape of the deflection curve for typical values of n and η_t.

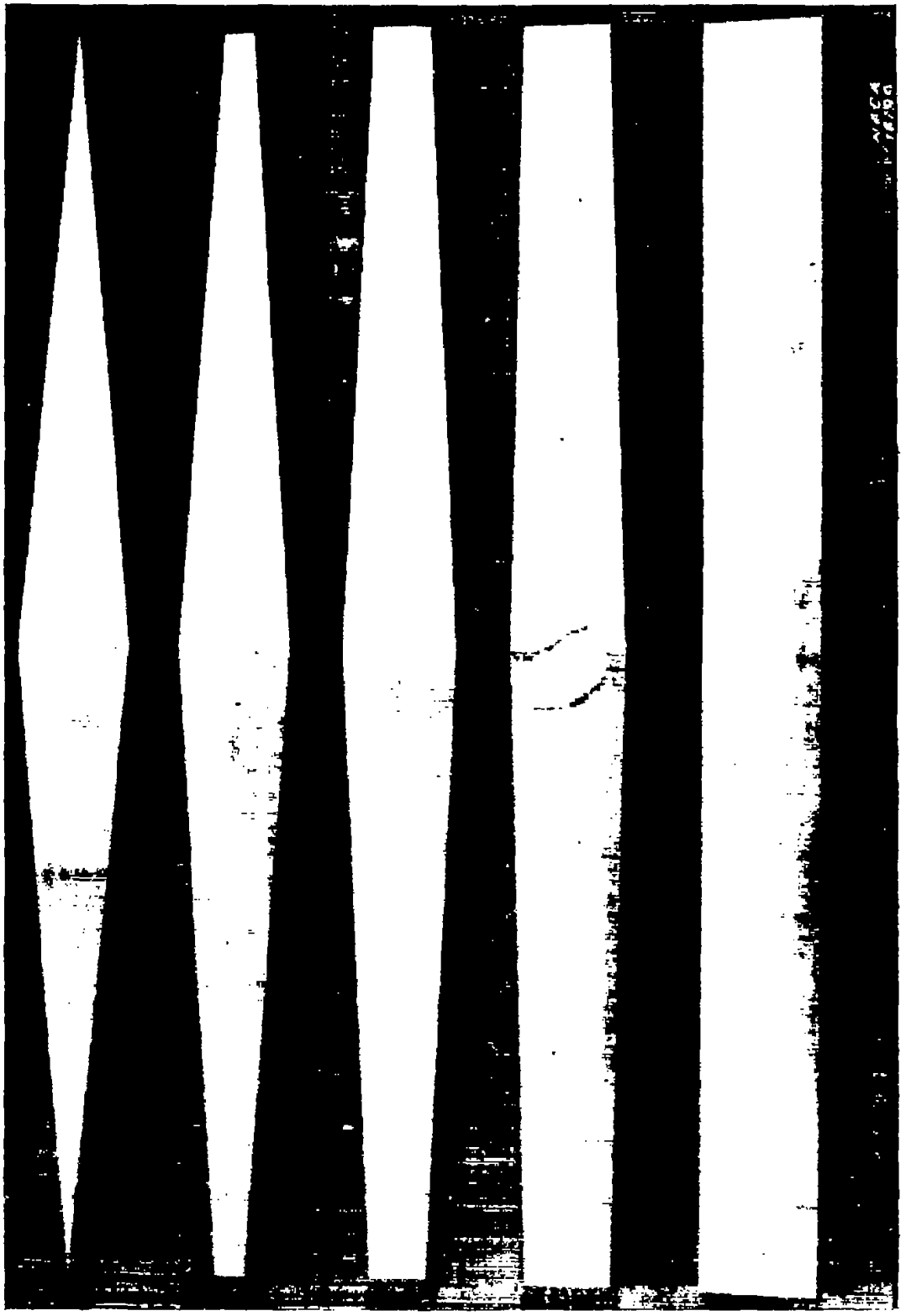

Figure 7.- Model beams tested.

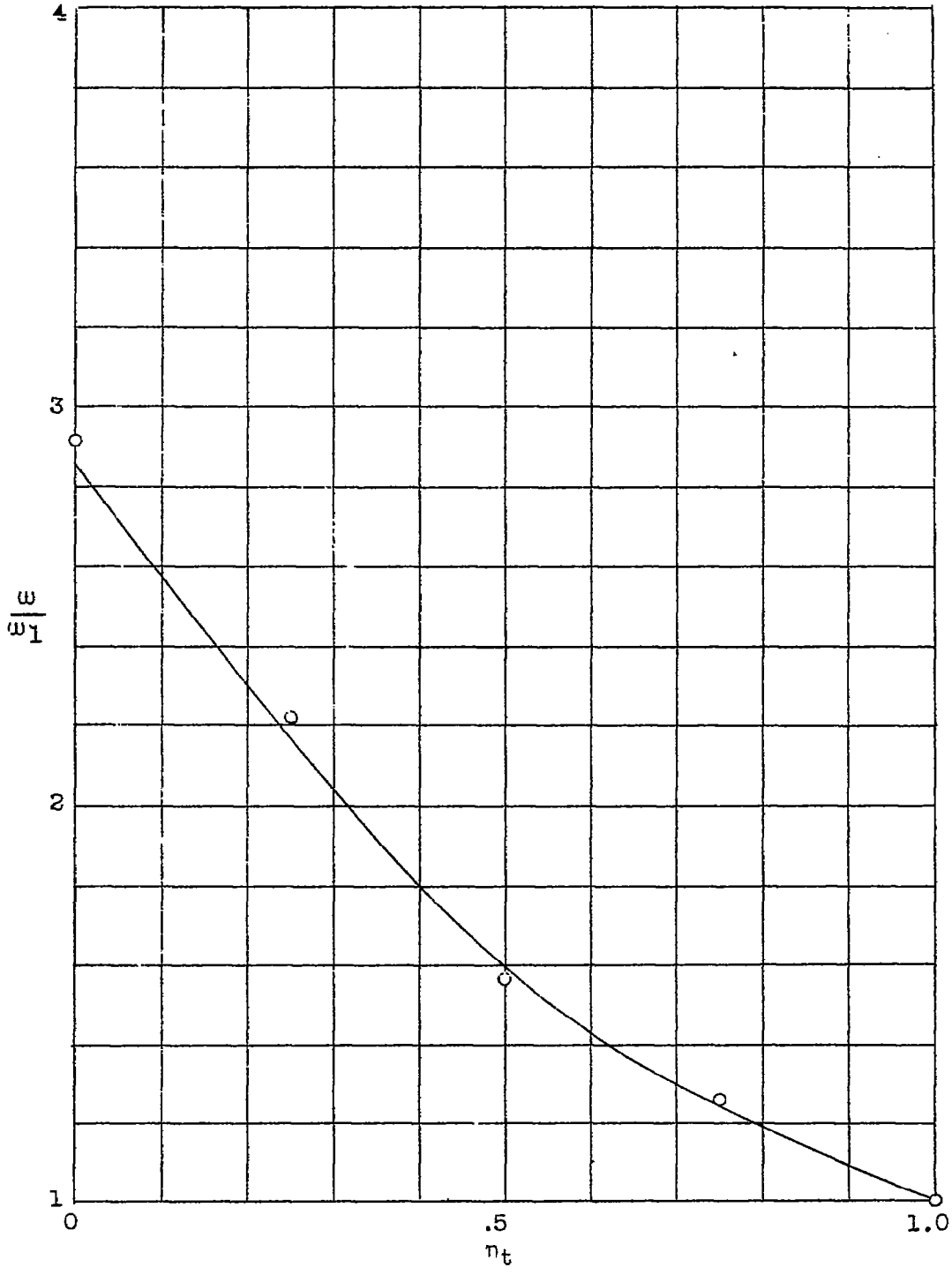

Figure 8.- Comparison of experimental values of frequency ratio with theoretical curve for n = 4.